

pubs.acs.org/JPCB Article

Blend Miscibility of Poly(ethylene terephthalate) and Aromatic Polyesters from Salicylic Acid

Hee Joong Kim, Xiayu Peng, Youngsu Shin, Marc A. Hillmyer,* and Christopher J. Ellison*



Cite This: J. Phys. Chem. B 2021, 125, 450-460



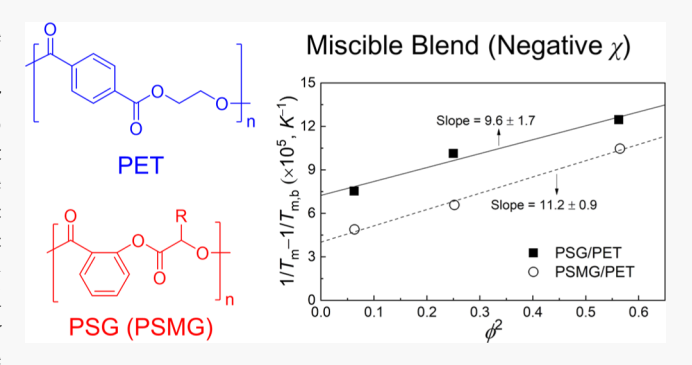
ACCESS

Metrics & More

Article Recommendations

Supporting Information

ABSTRACT: Poly(ethylene terephthalate) (PET) is one of the most prevalent polymers in the world due to its combined thermal, mechanical, and gas barrier attributes. Blending PET with other polymers is an appealing strategy to further tailor properties to meet the needs of an even more diverse range of applications. Most blends with PET are macrophase-separated; only a few miscible systems have been reported. Here, the miscibility of the aromatic polyesters poly(salicylic glycolide) (PSG) and poly(salicylic methyl glycolide) (PSMG) with PET is described. Both PSG and PSMG have similar chemical structures to PET but are derived from sustainable resources and readily degradable. This study suggests that they are fully miscible with PET over the entire



composition range, which is attributed to favorable interactions with PET. Negative polymer–polymer interaction parameters (χ) were determined using Flory–Huggins theory to describe melting temperature variations in the blends. In addition, the PET blends showed mechanical properties that are intermediate between the two homopolymers.

■ INTRODUCTION

Polymer blends have received considerable interest because the mixing of two or more polymers is one of the most costeffective and direct ways to tailor polymer properties. 1-4 However, most polymer pairs are immiscible due to their thermodynamic incompatibility. 1,2 The free energy of mixing $(\Delta G_{\rm m})$ depends on the enthalpy $(\Delta H_{\rm m})$ and entropy $(\Delta S_{\rm m})$ of mixing and $\Delta G_{\rm m}$ < 0 is required to form stable homogeneous polymer blends. Another necessary condition is that the second derivative of $\Delta G_{\rm m}$ with respect to composition should be negative to render a miscible blend at all compositions. $\Delta G_{\rm m}$ is generally dominated by $\Delta H_{\rm m}$ given that $\Delta S_{\rm m}$, while favorable, is negligible for high molar mass polymers. 5are a small number of polymer pairs with specific interactions between the polymer components that afford a homogeneous polymer blend (i.e., with $\Delta H_{\rm m}$ < 0). Hydrogen bonding,^{8–10} dipole–dipole interactions,¹¹ and ionic interactions¹² are the most common interactions found in homogeneous polymer blend systems. On the contrary, most polymer pairs do not possess these specific interactions and form macrophaseseparated morphologies.

Accordingly, there have been a limited number of commercialized miscible polymer blends such as poly-(phenylene oxide)/poly(styrene) (Noryl, SABIC), poly-(carbonate) (PC)/poly(acrylonitrile-styrene-acrylate) (Luran, BASF), poly(phenylsulfone)/poly(sulfone) (Acudel, Solvay Plastics), ethylene terpolymer/poly(vinyl chloride) (Alcryn, Advanced Polymer), and poly(vinylidene fluoride)/poly-(methyl methacrylate) (PMMA) (Polycast, Royalite). 13 Poly-

(ethylene terephthalate) (PET) is one of the most prevalent polymers worldwide, constituting approximately 10% of the global plastic market due to its thermal, mechanical, and oxygen barrier properties. ^{14,15} Blending PET with other polymers is an attractive strategy for augmenting this suite of properties, thus broadening application possibilities. For example, the elastic modulus of a PET/poly(butylene terephthalate) (PBT) (50/50 wt) blend is 1.25 times higher than those of pure PET and PBT. ¹⁶ However, only a few blend partners, such as PBT, ^{16,17} PC, ¹⁸ and poly(ether imides) ^{19,20} result in homogeneous blends with PET, and these blends are usually miscible only over limited composition ranges. This is likely because of the rapid crystallization of PET and strong PET–PET interactions. Therefore, it has been a significant challenge to develop PET-miscible polymers.

One possible strategy to produce PET-miscible polymers could be to develop polyesters with PET-like molecular structures. To date, significant effort has been devoted to exploring PET-like polyesters as potential alternatives to PET, sometimes with more sustainable characteristics, for example, poly(ethylene furanoate) (PEF),²¹ poly(dihydroferulic acid),²²

Received: October 14, 2020 Revised: November 28, 2020 Published: January 5, 2021





and poly(2-(2-hydroxyethoxy)benzoate).23 We,24 and others, 25,26 have also described PET-like polyesters known as poly(salicylic glycolide) (PSG) and poly(salicylic methyl glycolide) (PSMG); they are promising because of their sustainable origins, controllable polymerization processes, high glass-transition temperatures ($T_{\rm g} \approx 85$ °C), attractive mechanical properties ($E \approx 2.2 \text{ GPa}$), and facile hydrolytic degradation (e.g., complete degradation within a month at 50 °C in seawater). 24 However, most reported PET-like polyesters have not been evaluated for their potential miscibility with PET. Neves and co-workers prepared PEF/ PET blends (25-50 wt % PET) toward developing a sustainable and low processing cost blend system.²⁷ argued the miscibility of this system based on the visual transparency of the blends. However, no further experimental evidence was provided. For other PEF/PET blends (50/50 wt) prepared by the group of Papageorgiou, distinct T_{α} s of each homopolymer were observed, suggesting that PEF is not fully miscible with PET.²⁸

In this work, the miscibility of binary blends of PET with aromatic polyesters from salicylic acid (PSG and PSMG) was systematically investigated by thermal and optical analyses. The mechanical properties of the blends were also evaluated to better understand their potential utility. In addition to PET blends, the miscibility of poly(ethylene glycol-co-cyclohexanedimethanol terephthalate) (PETg) with PSG and PSMG was also examined because of the industrial importance of PETg; notably, the amorphous nature of PETg enables the production of clear and transparent products (e.g., protection film, food/medical packaging, and bottles) at lower processing temperatures while retaining most of the advantageous properties of PET.²⁹ PET/PSG, PET/PSMG, PETg/PSG, and PETg/PSMG blends were prepared and found to be miscible over the entire composition range. We conclude that the miscibility originates from specific weak interactions between the polymer pairs. This new experimental finding may provide opportunities for the development of PET-based polymer blends with diversified properties that also have the potential to be more sustainable.

EXPERIMENTAL SECTION

Materials. PSG $(M_{\rm n,NMR} \approx 11~{\rm kg~mol}^{-1})$ and PSMG $(M_{\rm n,NMR} \approx 19~{\rm kg~mol}^{-1})$ were synthesized by ring opening transesterification polymerization, as previously reported. High molar mass PSG $(M_{\rm n,NMR} \approx 87~{\rm kg~mol}^{-1})$ and PSMG $(M_{\rm n,NMR} \approx 91~{\rm kg~mol}^{-1})$ were also used to evaluate the mechanical properties of the blends. PET (Toray Industries, TC940, $M_{\rm n,SEC} = 29~{\rm kg~mol}^{-1}$, D = 2.3), PETg (Eastman Chemical Company, Spectar 14471, ethylene glycol:cyclohexanedimethanol = 2.2:1.0, $M_{\rm n,SEC} = 25~{\rm kg~mol}^{-1}$, D = 2.4), and poly(lactic acid) (PLA) (Nature works, 4060D, $M_{\rm n,SEC} = 100~{\rm kg~mol}^{-1}$, D = 1.2) were used after drying under reduced pressure at 60 °C for 2 days. Characterization data of PET and PETg are shown in Figures S1−S3. 1,1,1,3,3,3-Hexafluoro-2-propanol (HFIP) (Millipore Sigma) was used as received.

Preparation of Polymer Blends. To ensure blend homogeneity, each polymer pair was first dissolved in HFIP, yielding a 10 wt % polymer solution. The solution was stirred overnight at room temperature, cast on a Teflon mold, and dried on a bench-top overnight. Solid polymer films were obtained from the mold and further dried under reduced pressure at 60 °C. For larger scale blend preparation (>3 g),

the blends were obtained by precipitating a polymer solution from HFIP (10 wt %) into methanol.

Characterization. *Nuclear Magnetic Resonance Spectroscopy.* NMR spectroscopy data were obtained using a 500 MHz Bruker ADVANCE III HD spectrometer with a SampleXpress autosampler (HD-500). All NMR spectra were analyzed using TopSpin (Bruker) software.

Size Exclusion Chromatography. For determining the molar mass of PET and PETg, SEC was performed in 0.025 M potassium trifluoroacetate solution in HFIP (40 °C, 0.35 mL min⁻¹) on a Tosoh EcoSEC SEC system (HLC-8240GPC series liquid chromatograph) equipped with a refractive index detector and two HPLC columns (Tosoh TSKgel SuperAWM-H). Molar masses were determined by conventional calibration versus PMMA standards. Before SEC analysis, the dissolved polymer was filtered through a 0.2 μ m filter (Whatman).

Fourier-Transform Infrared Spectroscopy. FT-IR spectra of polymers and polymer blends were measured using a Nicolet 6700 FT-IR spectrometer in ATR mode by an MCT-A detector (Thermo Fisher Scientific). Spectra were taken with a resolution of 2 cm⁻¹ and were averaged over 64 scans.

Differential Scanning Calorimetry. DSC analyses were performed using a Mettler Toledo DSC 1 instrument in dry nitrogen. Approximately 5 mg of sample was loaded into hermetically sealed aluminum pans. Samples were heated at 10 $^{\circ}$ C min $^{-1}$ to 275 $^{\circ}$ C and held for 5 min to ensure complete PET melting and then cooled at -10 $^{\circ}$ C min $^{-1}$ to 0 $^{\circ}$ C and held for 5 min. Then, the samples were reheated (i.e., second heating) at 10 $^{\circ}$ C min $^{-1}$ to 275 $^{\circ}$ C. The glass-transition temperature ($T_{\rm g}$) was determined as the midpoint of the specific heat increment. $^{30-32}$

The melting temperature $(T_{\rm m})$ was determined as the endotherm peak value following the guidance of the International Conference on Thermal Analysis and Calorimetry. 33,34 Given that some samples showed a broad melting range, the melting peak temperature better represents the melting character as opposed to other characteristic temperatures (e.g., onset of melting, endset of melting, etc.). 33,34 In the case of two overlapping melting endotherms, the major (larger) melting peak temperature was taken as the $T_{\rm m}$ because it is closer to the equilibrium $T_{\rm m}$. $^{35-38}$ Although the determination of equilibrium $T_{\rm m}$ by a Hoffman—Weeks extrapolation is one of the most accurate methods, 8,30,39 here $T_{\rm m}$ was determined without an annealing step due to some thermal degradation of PSG and PSMG during long anneals at high temperatures. A detailed discussion can be found in the manuscript.

To investigate the crystallization behavior of the blends, the samples were annealed at 275 °C and either quenched at about $-200~^{\circ}\mathrm{C}~\mathrm{min^{-1}}$ to about $-30~^{\circ}\mathrm{C}$ or slowly crystallized ($-3~^{\circ}\mathrm{C}~\mathrm{min^{-1}}$ to 220 °C and then held isothermally at 220 °C for 5 min), and finally cooled at $-10~^{\circ}\mathrm{C}~\mathrm{min^{-1}}$ to 0 °C. Then, samples were reheated at 10 °C min $^{-1}$ to 275 °C, and the $T_{\rm g}$ and $T_{\rm m}$ values were determined as described earlier.

Optical Microscopy. Polymer blends were observed using a polarized optical microscope (OLYMPUS, BX-53) with a 20× objective (OLYMPUS, numerical aperture = 0.40, working distance = 1.2 mm) equipped with a LINKAM stage for temperature control. To observe phase homogeneity, the polymer blends were melted on a microscope stage at 270 °C, covered by a glass cover slip, and images were collected every 30 s using an integrated CCD camera and crossed polarizers. To observe crystallization, the polymer blends were melted at 270 °C followed by cooling at -50 °C min⁻¹ to 220 °C. The

samples were then crystallized isothermally at 220 $^{\circ}$ C. Note that the crystallization temperature (220 $^{\circ}$ C) was chosen such that both PET and PET blend crystallization could be observed under the same conditions.

X-ray Diffraction. X-ray diffraction (XRD) patterns were measured on a Bruker D8 DISCOVER 2D with monochromatic Co K α radiation (λ = 1.78899 Å). Signals were collected with a 2D detector and converted to a 1D signal by azimuthal integration. 2 θ values were converted to a Cu K α source (λ = 1.5418 Å). Scan time was set to 300 s.

Density Measurements. Both PSG and PSMG were compression-molded (150 °C for 2 min followed by quenching) to prepare dense polymer films. The density of the polymer films was measured by Archimedes' principle with a density determination kit for Excellence XP/XS analytical balances (Mettler Toledo). The density measurements at room temperature for each polymer were repeated at least 10 times to obtain an average value. The density values of PSG and PSMG were found to be 1.337 and 1.333 g cm⁻³, respectively. Note that the density of PET is dependent on crystal content. As-received PET pellets were used and the measured density was 1.342 g cm⁻³, consistent with reported values of mostly amorphous PET. 17,40

Refractive Index Measurements. Polymer samples were compression-molded (Wabash Carver press, IN, USA) in between Teflon sheets above their $T_{\rm g}$ or $T_{\rm m}$ for 1 min and quenched to make an amorphous film. Clear and transparent films were cut out, resulting in samples with approximately 5 mm length, 10 mm width, and <100 μ m thickness. The refractive indices of the samples were measured by an Abbé refractometer. The measurements were conducted at least 5 times from multiple samples. The refractive indices of PET (mostly amorphous), PETg, PLA, PSG, and PSMG were 1.594 \pm 0.007, 1.545 \pm 0.006, 1.517 \pm 0.010, 1.528 \pm 0.026, and 1.536 \pm 0.013, respectively. Note that the refractive index measurement of molten samples was not possible due to the potential damage to the equipment at a high temperature (>270 °C).

Mechanical Properties. Polymer blend samples were compression-molded (Wabash Carver press, IN, USA) in between Teflon sheets at 270 °C for 1 min. To minimize the air bubbles in the sample, minimal pressure (≈300 lbs force) was first applied for 40 s, which was then increased to ≈500 lbs force, which was maintained for 20 s. Then, the sample was rapidly quenched to ≈40 °C using water cooling. Dog-bone-shaped specimens were cut out, resulting in samples with approximately 0.2 mm thickness, 5 mm gauge width, and 20 mm gauge length (ASTM D1708). Samples were tensile tested to the point of break with an extension rate of 5 mm min⁻¹ at room temperature using a Shimadzu Autograph AGS-X Tensile Tester (ASTM D1708 protocol).

■ RESULTS AND DISCUSSION

Thermal Analyses: Glass-Transition Temperature $(T_{\rm g})$. Four different sets of polymer blends, that is, PET/PSG, PET/PSMG, PETg/PSG, and PETg/PSMG, were prepared by solution mixing (See Figure 1 for the chemical structures of each polymer). In addition, other polymer blends (PET/PLA and PETg/PLA) were prepared as immiscible control samples. DSC analyses of the polymer blends were carried out: the observation of a single $T_{\rm g}$ in a binary blend is the most common method for establishing the miscibility of a polymer pair. $^{1,41-43}$ Figure 2 shows the glass transition region in the

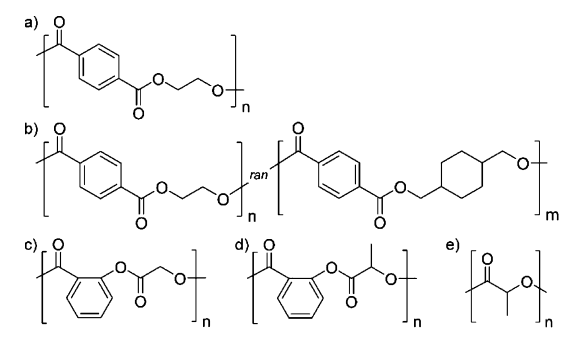


Figure 1. Chemical structures of (a) PET, (b) PETg (n:m = 2.2:1.0), (c) PSG, (d) PSMG, and (e) PLA.

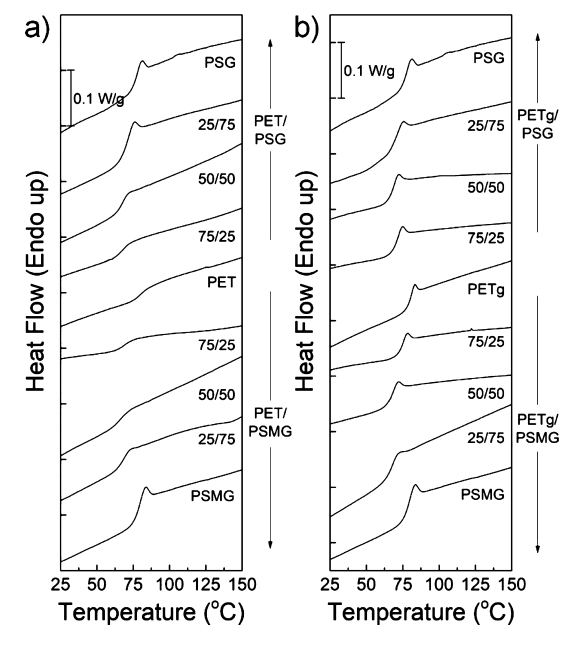


Figure 2. Glass-transition region in the DSC data (second heating, 10 °C min⁻¹): (a) PET/PSG (or PSMG) blends and (b) PETg/PSG (or PSMG) blends. The thermograms are shifted vertically for clarity.

DSC data of polymer blends with different compositions. All the polymer blends displayed single $T_{\rm g}$ s, suggesting that PSG and PSMG are fully miscible with PET and PETg in the amorphous region over the entire composition range. In contrast, two distinct $T_{\rm g}$ s were observed in the immiscible PET/PLA (50/50 wt) and PETg/PLA (50/50 wt) samples (Figure S4). The $T_{\rm g}$ s of the miscible polymer blends were lower than those of the homopolymers, likely due to the specific interactions between the two different polymers as will be discussed later. Note that 13 C NMR spectra of as-prepared and compression-molded (at 270 °C) samples confirmed no significant interchain transesterification reactions (Figure S5).

Various theoretical and empirical equations have been established to describe the $T_{\rm g}$ of miscible polymer blends (e.g., Fox, Gordon-Taylor, Kwei, and Lu–Weiss equations). S,43,44 Given that the present blends exhibit a $T_{\rm g,blend}$ that is lower than the $T_{\rm g}$ of each homopolymer, the Kwei equation (eq 1) is relevant because it can capture $T_{\rm g,blend}$ with large positive or negative deviations compared to the homopolymer $T_{\rm g}$ s (Figure 3). The Kwei equation is written

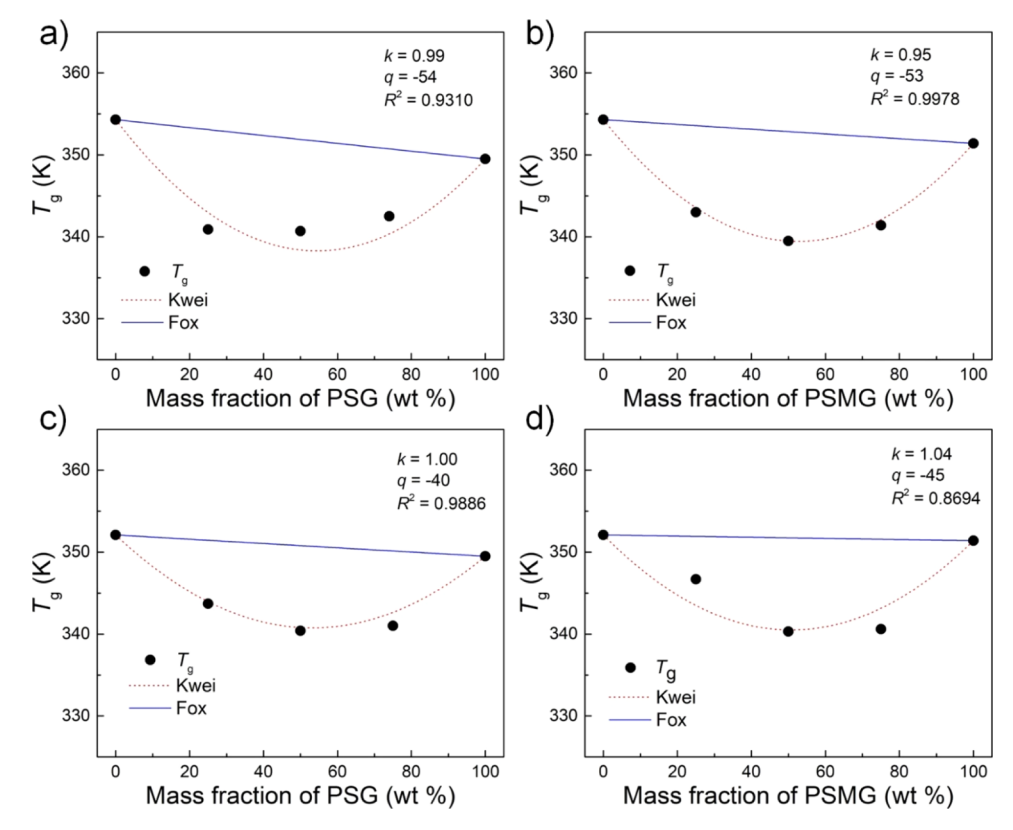


Figure 3. Plots of T_g vs composition based on experimental data (\bullet), the Fox equation (solid blue line), and the Kwei equation (dashed red line). (a) PET/PSG, (b) PET/PSMG, (c) PETg/PSG, and (d) PETg/PSMG. k and q values are the calculated constants in the Kwei equation, where R^2 is the coefficient of determination.

$$T_{\rm g} = \frac{w_1 T_{\rm g,1} + k w_2 T_{\rm g,2}}{w_1 + k w_2} + q w_1 w_2 \tag{1}$$

where w_1 and w_2 are the weight fractions of each component, $T_{g,1}$ and $T_{g,2}$ are the corresponding T_{g} s of each homopolymer component, and k and q are fitting constants. The k and qvalues were obtained by a nonlinear least squares fitting of the equation to the experimental data. 8,30 The k value is associated with the strength of specific attractive interactions in a polymer blend: a larger k indicates stronger attractive interactions between different polymer chains. ^{8,45,46} In general, $k \approx 1$ was obtained for all the polymer blends in this study. In comparison, lower k values have been reported for poly(phenyl methacrylate)/poly(ethylene oxide) (PEO) $(k = 0.15-0.45)^{47}$ and poly(acetoxystyrene) (PAS)/PEO (k = 0.14)³⁰ blends, and a higher k value was reported for poly(vinylphenol-comethyl methacrylate) (PVP-MMA)/PEO blend (k = 4.0). Therefore, the specific interaction strengths in PET (or PETg)/PSG (or PSMG) blend systems are moderate as compared to the above example blends. This is likely because the blend systems in this study do not contain strong hydrogen bond donors (e.g., hydroxy) such as those in PVP-MMA/PEO blends but include more C=O bonds than PAS/PEO blends, which could enhance intermolecular interactions.

The *q* parameter is thought to quantify the excess energy by which the weight average stabilization of the polymer in the blends is greater than the weight average stabilization of the polymer in the homopolymers. In other words, *q* provides information for the relative importance of intrachain-associated and interchain-associated interactions. A positive *q* value indicates that the polymers are better stabilized by blending,

which is attributed to stronger interchain interactions than self-associated interactions, leading to higher $T_{\rm g}$ in the blends. A negative q value suggests that the polymer stabilization energy in the blends is smaller than the stabilization energy of the homopolymers. This means that the self-associated interactions are stronger than interchain interactions, typically resulting in an increase in free volume and lower $T_{\rm g}$ in the blends. $^{46,48-50}$ For PET (or PETg)/PSG (or PSMG) blend systems, negative q values (\approx -50) were obtained, suggesting that self-associated interactions (e.g., PET-PET) are stronger than interchain interactions (e.g. PET-PSMG). In comparison, the q values in the PET (or PETg)/PSG (or PSMG) blend systems are larger than those of other miscible polymer blends such as phenolic resin/PAS (q=-245) and phenoxy resin/poly(ε -caprolactone) (PCL) (q=-100) blend systems have more interchain interactions.

Similar trends for blend $T_{\rm g}$ values were observed for the polymer blends with a high molar mass PSG $(M_{\rm n,NMR} \approx 87~{\rm kg}~{\rm mol}^{-1})$ and PSMG $(M_{\rm n,NMR} \approx 91~{\rm kg}~{\rm mol}^{-1})$; single $T_{\rm gblend}$ s were observed and lower than the $T_{\rm g}$ of each homopolymer (Figures S6 and S7). By fitting $T_{\rm g,blend}$ values using the Kwei equation, k and q values were evaluated (Figure S8). In general, $k \approx 1.1$ was obtained for the polymer blends with a high molar mass PSG and PSMG, which is comparable to those of the polymer blends with a lower molar mass PSG and PSMG (Figure 3). This is because the interaction strength between a polymer pair (e.g., PET-PSMG) is almost independent of molar mass. In contrast, the obtained q values (between -86 and -73) were lower than those of the polymer blends with a lower molar mass PSG and PSMG. This

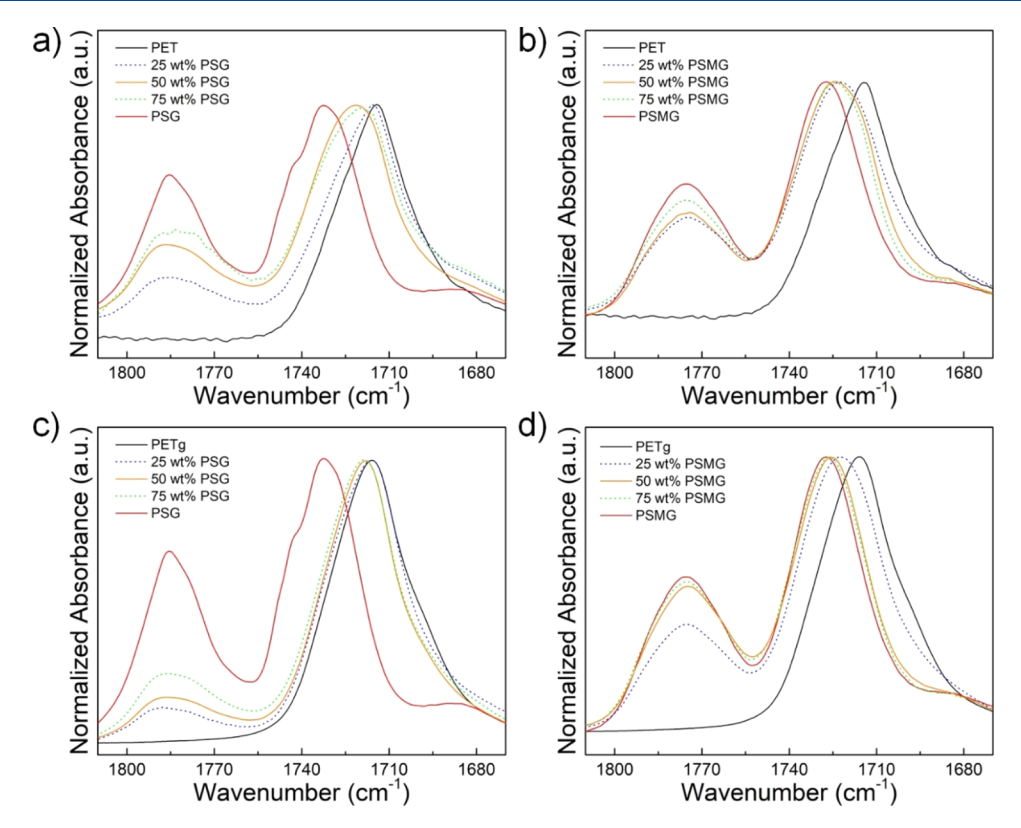


Figure 4. Expanded FT-IR spectra of the polymer blend corresponding to the carbonyl region. (a) PET/PSG, (b) PET/PSMG, (c) PETg/PSG, and (d) PETg/PSMG.

indicates that the relative strength of self-associated interactions compared to interchain-associated interactions increases with increasing molar mass of PSG and PSMG, possibly due to a decrease in chain mobility and free volume that occurs with increasing molar mass/decreasing density of chain ends. 8,53

FT-IR Analysis. Interchain-associated interactions in the polymer blends were investigated by FT-IR. Figure 4 shows the expanded FT-IR spectra of the polymer blends corresponding to the carbonyl stretching region. PET and PETg both showed single carbonyl stretching at 1714 and 1716 cm⁻¹, respectively. PSG (1732 and 1785 cm⁻¹) and PSMG (1727 and 1775 cm⁻¹) displayed two carbonyl stretching peaks, which could be attributed to the two different ester linkages (Ph-CO-O-C and Ph-O-CO-C). The carbonyl bands of PSG (or PSMG) near 1730 cm⁻¹ and PET (or PETg) near 1710 cm⁻¹ are broadened and shifted upon blending. This is likely because of the presence of interchain-associated interactions; other studies have shown broadening and/or shifting of a band near 1720 cm⁻¹ corresponding to the interactions of carbonyl groups. ^{8,42,52,54} A gradual change indicates that the distribution of the interchain-associated species is dependent on the composition of the mixture.8 The other carbonyl bands of PSG at 1785 cm⁻¹ and PSMG at 1775 cm⁻¹ are almost constant, indicating that a carbonyl group connected with a phenoxide group (Ph-O-CO-C) is relatively uninvolved. We postulate that this is because the oxygen atom in the carbonyl group (Ph-O-CO-C) is less electron-rich than that in the other carbonyl group (Ph-CO-O-C); the 13C NMR spectrum of PSMG indicates that the carbon atom in the former carbonyl group (Ph-O-CO-C) is more deshielded (stronger electron withdrawing) than that in the latter carbonyl group (Ph-CO-O-C) (Figure S5). It is worth noting that the broadness and peak

position of the carbonyl bands of the blends were different from those of linear combinations of the individual polymers weighted by the composition, further confirming that interchain interactions develop upon blending (Figure S9). In addition, $-CH_2-$ (or $-CH_3$) bending (1381 and 1415 cm⁻¹) vibrations shifted and broadened when blended (Figure S10), indicating that alkyl groups might partially contribute to the weak interchain interactions. Similar weak interactions of carbonyl and methylene groups were observed in the PAS/PEO blend.³⁰ This result is also consistent with the aforementioned $k \approx 1$ (weak attractive interactions between a polymer pair). In addition, the interaction between two different polymer chains could partially reduce self-associations, contributing to the aforementioned increase in free volume and decrease in T_o s (q < 0).

Thermal Analyses: Melting Temperature (T_m) . The depression of crystallization of a semicrystalline polymer is additional strong evidence of miscibility. 8,9,30,54,55 If a semicrystalline polymer is miscible with an amorphous polymer in the molten state, the chemical potential of the semicrystalline polymer decreases due to dilution by the miscible amorphous polymer, resulting in melting temperature depression. Figure 5 shows melting endotherm peaks of PET and PET blends in the DSC data. The two melting peaks of PET are likely due to either two distinct crystal populations^{35,56} or heat-crystallization phenomena.^{36,37} The number and shape of melting endotherm peaks of PET are dependent on various parameters such as heating rate, annealing time and temperature, and crystallinity. ^{36–38,57} In this study, the melting peak temperature of the major (larger) peak was taken as the $T_{m,PET}$ because it is closer to the equilibrium $T_{\rm m,PET}~(\approx 250~{\rm ^{\circ}C})$ and known to be constant over large variations in conditions (e.g., annealing time and temperature). 36,37,56 Increasing the PSG or PSMG

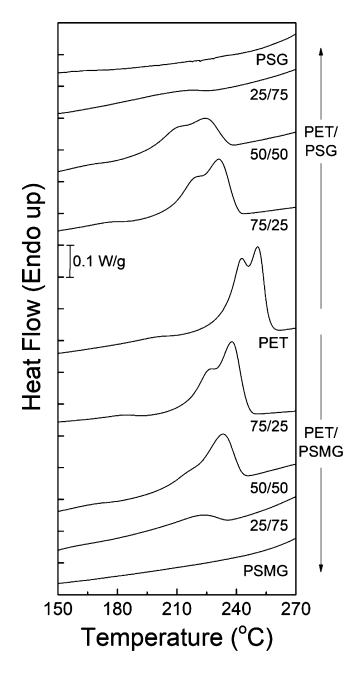


Figure 5. Melting temperature region in the DSC data (2nd heating, 10 °C min⁻¹) for PET/PSG and PET/PSMG blends. The thermograms are shifted vertically for clarity.

content led to a decrease in $T_{\rm m,PET}$ and crystallinity of PET, suggesting that PET is miscible with both PSG and PSMG. This is likely because PSG and PSMG polymer chains interact with PET on the molecular level, thereby reducing the chemical potential of the crystallization of PET. In contrast, there is no evidence of $T_{\rm m,PET}$ depression when PET is blended with PLA (50/50 wt.) due to their immiscibility (Figure S4). Thermodynamic parameters, such as the polymer–polymer interaction parameter (χ), can also be evaluated from these data; the depressions in $T_{\rm m,PET}$ were further analyzed by using the Flory–Huggins theory (eq 2)^{41,58,59}

$$\frac{1}{T_{\rm m}} - \frac{1}{T_{\rm m,b}} = -\frac{RV_2}{\Delta H_2 V_1} \left[\frac{\ln \phi_2}{x_2} + \left(\frac{1}{x_2} - \frac{1}{x_1} \right) (1 - \phi_2) \right] + \chi_{12} (1 - \phi_2)^2$$
(2)

where $T_{\rm m}$ is $T_{\rm m,PET}$ (524 K), $T_{\rm m,b}$ is $T_{\rm m}$ of the polymer blend, R is the universal gas constant (8.314 J mol⁻¹ K⁻¹), V is the molar volume of the repeating units of the polymer ($V_{\rm PET} = V_{\rm PSG} = 143.41~{\rm cm}^3~{\rm mol}^{-1}, V_{\rm PSMG} = 133.94~{\rm cm}^3~{\rm mol}^{-1}$), ΔH_2 is the heat of fusion for 100% crystalline PET (26.9 kJ mol⁻¹), ⁶⁰ Φ is the volume fraction of the component in the polymer blend, x is the degree of polymerization of each polymer component, and χ_{12} is the interaction parameter. The subscripts 1 and 2 represent the amorphous polymers (PSG or PSMG) and PET, respectively. The terms related to x_1 and x_2 can be neglected given that those values are very small for high molar mass samples. ^{8,30,54,55} This yields a simple equation (eq 3)

$$\frac{1}{T_{\rm m}} - \frac{1}{T_{\rm m,h}} = -\frac{RV_2}{\Delta H_2 V_1} \chi_{12} \phi_1^2 \tag{3}$$

Figure 6a shows the linear relationship between $T_{\rm m,PET}$ depression and the volume fraction of an amorphous polymer

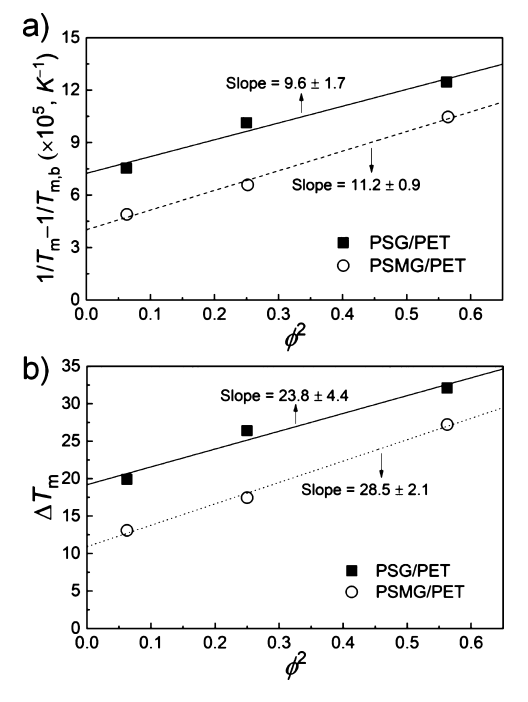


Figure 6. (a) Flory—Huggins Plots and (b) Nishi—Wang plots of the PET blends. Φ indicates the volume fraction of PSG or PSMG in the blends.

(i.e., the Flory-Huggins plots). The negative polymerpolymer interaction parameters ($\chi_{PSG,PET} = -0.31$, $\chi_{PSMG,PET}$ = -0.36) were calculated from the slopes in Figure 6a, confirming that both PSG and PSMG are thermodynamically miscible with PET. The calculated χ values of the blends are comparable to χ values of other miscible polyester blends that are calculated from $T_{\rm m}$ depressions, for example, χ of PCL/ poly(vinyl chloride) $\approx -0.3^{41}$ and PBT/polyarylate $\approx -0.4^{61}$ It is worth noting that these estimated χ_{12} parameters do not account for entropic parameters such as architectural and conformational effects. 62 The interaction energy density (B_{12}) is another important parameter because it is independent of how statistical segments are defined while χ_{12} is not. 62 This provides clearer information for the comparison of the interaction strength per unit volume. B_{12} can be calculated by substituting eq 4 into eq 3, yielding the Nishi-Wang equation (eq 5)^{55,59}

$$B_{12} = \frac{RT_{\rm m}\chi_{12}}{V_{\rm l}} \tag{4}$$

$$T_{\rm m} - T_{\rm m,b} = -T_{\rm m} \frac{B_{12} V_2}{\Delta H_2} \phi^2 \tag{5}$$

Negative B_{12} values ($B_{\rm PSG,PET} = -8.5~{\rm J~cm^{-3}}$, $B_{\rm PSMG,PET} = -10~{\rm J~cm^{-3}}$) were obtained from the Nishi–Wang plots (Figure 6b), further confirming that the blends are miscible. Note that B_{12} values can be also directly calculated from eq 4 ($B_{\rm PSG,PET} = -9.4~{\rm J~cm^{-3}}$, $B_{\rm PSMG,PET} = -11~{\rm J~cm^{-3}}$), which are close to those determined from the Nishi–Wang plots. The absolute values of the interaction energy density are smaller than those of polymer blends with strong hydrogen bonding (e.g., PVP-MMA/PEO blend, $B_{12} = -29.23~{\rm J~cm^{-3}})^8$ but comparable to those of polymer blends with weak interactions (e.g., PAS/PEO blend, $B_{12} = -6.64~{\rm J~cm^{-3}})^{.30}$ These

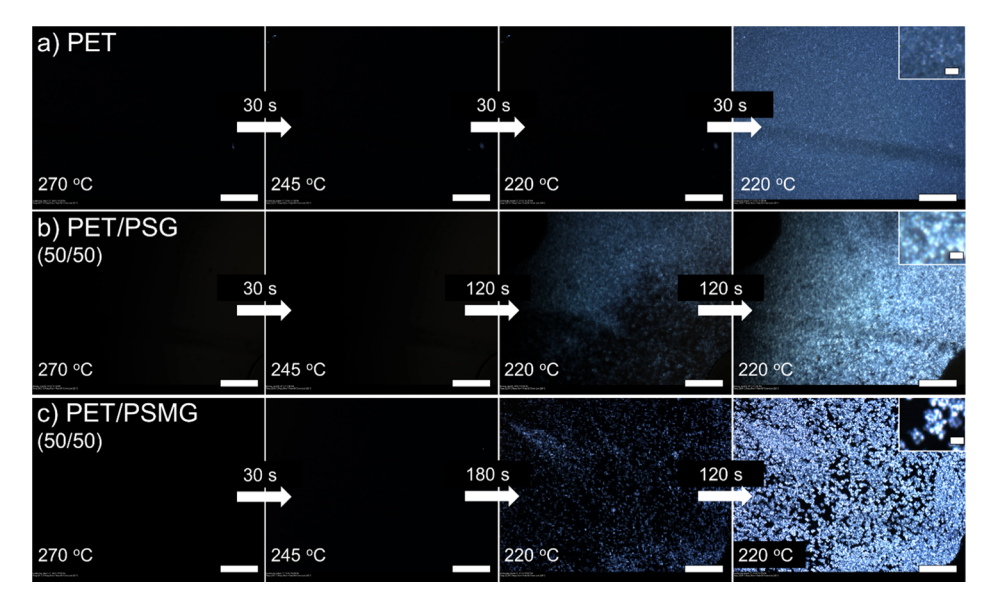


Figure 7. Polarized optical microscope images upon crystallization. The sample stage was cooled at -50 °C min⁻¹ from 270 to 220 °C, followed by isothermal crystallization at 220 °C (Scale bar = 1 mm, inset scale bar = 0.1 mm). See Figures S16 and S17 for more images.

comparisons are consistent with the aforementioned \boldsymbol{k} value comparisons.

In addition, $T_{\rm m}$ depressions as well as broadening of melting endotherms were observed for the polymer blends with high molar mass PSG and PSMG (Figure S11), further suggesting that PET is miscible with the high molar mass polymers. The negative polymer–polymer interaction parameters ($\chi_{\rm PSG,PET} = -0.67$, $\chi_{\rm PSMG,PET} = -0.55$) and the negative interaction density values ($B_{\rm PSG,PET} = -19~\rm J~cm^{-3}$, $B_{\rm PSMG,PET} = -15~\rm J~cm^{-3}$) were calculated by the Flory–Huggins and the Nishi–Wang plots, respectively, confirming that the blends are miscible (Figure S12). The absolute χ_{12} and B_{12} values of the blends with high molar mass PSG and PSMG are larger than those with low molar mass PSG and PSMG. This is probably due to the contribution of entropic terms (the terms related to x_1 and x_2 in eq 2); these values decrease with increasing molar mass (x_1 and x_2). 63

Optical Analysis. The optical clarity of the polymer blends was examined by optical microscopy (OM) to directly visualize phase homogeneity, another indicator of miscibility. When the PET (or PETg)/PSG (or PSMG) blends were melted on the heating stage, homogeneous samples were observed, indicating miscibility (Figures S13 and S14). In contrast, clear phase boundaries (phase heterogeneity) were observed for PET (or PETg)/PLA blends (Figure S15), confirming immiscibility. This is consistent with the phase contrast for other immiscible blends, PC/poly(styrene)⁶⁴ and PET/PEF. Given that refractive indices of the polymer pairs are different (see the Experimental section for specific values), the phase homogeneity/contrast are attributed to miscibility/immiscibility.

The dimensions of the crystallites and the crystallization rates were visually investigated by OM with crossed polarizers (Figure 7). The melted blend samples were cooled at -50 °C min⁻¹ from 270 to 220 °C, followed by isothermal crystallization at 220 °C. PET showed rapid crystallization (30 s of isothermal crystallization), forming small crystallites (Figure 7a). In comparison, the crystallization rate of PET blends was slower than that of PET, and the formed crystallites were larger than those of PET (Figure 7b,c). The

crystallization rate decreased and crystallite size increased with increasing PSG or PSMG content (Figures S16 and S17). In general, the crystallization rate is represented as the product of a transport term (kinetic factor) and driving force term (thermodynamic factor). 65,66 The decrease in T_g of the blends leads to a higher chain mobility at the crystallization temperature, thereby facilitating crystallization (kinetic factor), but the crystallization is less thermodynamically favorable for the blends due to the dilution of the crystallizable component in the molten state (thermodynamic factor). For the PET blends with PSG or PSMG, we speculate that the slow crystallization rate is likely because the thermodynamic factor is more dominant than the kinetic factor. Decreases in crystallization rate have been observed in other miscible amorphous/semicrystalline polymer blends. 30,67,68 In addition, being less thermodynamically favorable, the blends could form fewer nucleation sites, eventually growing into lager crystallites. Reduction in the surface free energy of chain folding (or crystallization activation energy) could also contribute to the formation of larger crystallites. 69 In addition, the crystallites in the polymer blends were uniformly distributed over the entire area, which is an additional signature of miscible binary blend systems.

Another hypothesis for the changes in crystallization behavior upon blending is that PSG or PSMG could be incorporated into the PET crystallites or cocrystallize with PET during slow crystallization. To test this hypothesis, DSC experiments were performed on blends after quenching at \approx -200 °C min⁻¹ and slow cooling at −3 °C min⁻¹ (Figure S18). For PET, the $T_{\rm m}$ s after quenching and slow cooling were identical, indicating that PET itself can readily crystallize under both crystallization conditions. For PET/PSG and PET/ PSMG blends, the $T_{\rm m}$ after slow cooling was lower than that after quenching, indicating that the compositions or structures in the crystallites are dependent on crystallization conditions. We speculate that PSG or PSMG could distort PET crystallites or cocrystallize with PET only under slow crystallization conditions. It is also worth noting that PSG itself showed $T_{\rm m} \approx$ 125 °C during the first heating cycle but the melting endotherm disappeared in the second heating cycle, likely due to slow crystallization. ²⁴ In addition, the T_{σ} s of the blends after quenching and slow cooling were not significantly different, indicating that the compositions in the amorphous regions are similar (See Figure 3). This is likely because the PSG or PSMG chains are possibly incorporated in the crystallites during the slow crystallization, thereby maintaining the amorphous PET/PSG (or PET/PSMG) ratio. The DSC results were corroborated by XRD profiles (Figure S19). The 2θ peaks at 17.5, 21.6, and 26.0° in PET were slightly shifted for slowly crystallized PET/PSG and PET/PSMG blends, suggesting that the crystal lattice is slightly distorted by the possible incorporation of PSG (or PSMG) chains. Similar peak shifts of miscible polymer blend systems in XRD profiles have been attributed to the cocrystallization behavior. 70-72 Note that XRD profiles of quenched samples did not allow a more detailed analysis of the crystalline state post quenching (Figure S19b). These DSC and XRD data support the hypothesis that the PSG or PSMG component is likely incorporated into PET crystallites under a slow crystallization condition.

Mechanical properties. In order to better understand the potential utility of these blends, the mechanical properties of PET and PET blends with high molar mass PSG and PSMG were evaluated by tensile testing (ATSM D1708 protocol). Note that the PET blends containing low molar mass PSG and PSMG were brittle with poor mechanical properties. The representative strain-stress data for PET and PET blends are displayed in Figure 8 (see Figure S20 for individual strain-

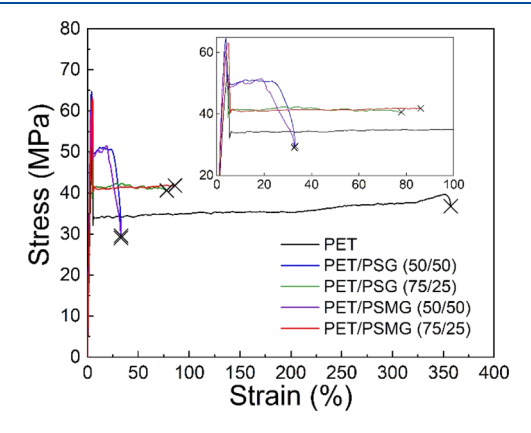


Figure 8. Representative strain-stress data of PET and PET blends.

stress data), and the associated mechanical properties are summarized in Table 1. The PET blends displayed a tensile strength of $\sigma \approx 60$ MPa and elastic modulus of $E \approx 2$ GPa, which are between those of PET and PSG (or PSMG). In

Table 1. Mechanical Property Data of PET and PET Blends Measured by Tensile Testing

sample	composition (wt)	tensile strength (MPa)	elongation at break (%)	modulus (GPa)
PET/PSG	50/50	63.7 ± 2.0	36 ± 18	2.0 ± 0.2
	75/25	60.3 ± 1.2	84 ± 6.3	2.0 ± 0.0
PET/PSMG	50/50	60.4 ± 2.8	36 ± 11	2.2 ± 0.1
	75/25	61.1 ± 3.3	85 ± 12	2.1 ± 0.3
PET		52.2 ± 2.1	360 ± 7.3	1.6 ± 0.1
PSG or PSMG ^a		64.4 ± 3.2	4.7 ± 0.3	2.3 ± 0.1

^aReported values.²⁴

general, the mechanical properties of the miscible blends are between those of the two homopolymers and proportional to the ratio of the polymer pair. ^{67,73,74} The elongations at break values of the PET blends ($\varepsilon_{\rm b} \approx 36\%$ and 85% for the blends of 50 wt % PET and 75 wt % PET, respectively) were lower than that of PET ($\varepsilon_{\rm b}$ = 360%). This is attributed to the relatively large entanglement molar masses of PSG and PSMG ($M_{\rm e,PSG}$ = 5.7 kg mol⁻¹, $M_{e,PSG} = 4.8 \text{ kg mol}^{-1}$); ²⁴ the dilution of chain entanglements promotes failure at lower elongations. Still, these properties are competitive with other miscible polyester blends used for applications such as textiles and engineering components; PET/PC ($\sigma \approx 60$ MPa, $\varepsilon_{\rm h} \approx 50\%$, Makroblend, Bayer) and PBT/PC/elastomer ($E \approx 2.5$ GPa, $\varepsilon_{\rm h} \approx 50\%$, Ultrablend, BASF) are currently used in those applications. ^{13,40,75} Moreover, blending PET with PSG or PSMG could lead to improved processability given the relatively lower $T_{\rm m}$ with the added benefit of sustainability introduced by PSG and PSMG. In addition, the mechanical properties of the PET blends provide additional evidence of their miscibility. Generally, immiscible polymer blends possess poor mechanical properties due to the macrophase separation and poor interfacial adhesion of such a polymer pair.^{2,13} For example, the PET blend with \approx 10 wt % polyethylene (PE) showed a small elongation at break (ε < 15%), which is substantially smaller than those of parent homopolymers ($\varepsilon_{\rm b,PET} \approx 300\%$, $\varepsilon_{\rm b,PE} \approx 800\%$). The PET blends were not brittle and their mechanical properties were between those of the two homopolymers. This strongly supports the notion that there is no macrophase separation in these blends.

CONCLUSIONS

pubs.acs.org/JPCB

Four different binary blends, that is, PET/PSG, PET/PSMG, PETg/PSG, and PETg/PSMG, were prepared. These binary systems are fully miscible over the entire composition range, confirmed by a single $T_{\rm g}$ in DSC, depression in $T_{\rm m,PET}$, and phase homogeneity in OM images. This is attributed to the interactions between the polymer pairs, confirmed by FT-IR analysis. A negative interaction parameter (χ) and interaction energy density (B) were estimated based on the depression in T_{m,PET} using Flory-Huggins theory and the Nishi-Wang equation. In addition to the depression in $T_{m,PET}$, PSG and PSMG are likely incorporated into PET crystallites under slow crystallization conditions (-3 °C min⁻¹). PET blends exhibited mechanical properties that are between those of two homopolymers. Blending PET with PSG or PSMG could potentially improve the processability and sustainability. These findings provide insight into the development of PET-based blends from sustainable materials for future advanced polymeric materials.

ASSOCIATED CONTENT

Supporting Information

The Supporting Information is available free of charge at https://pubs.acs.org/doi/10.1021/acs.jpcb.0c09322.

> ¹H and ¹³C NMR data, additional DSC data, additional FT-IR spectroscopy data, OM images, additional polarized OM images, XRD data, and additional stress-strain curves (PDF)

AUTHOR INFORMATION

Corresponding Authors

Marc A. Hillmyer – Department of Chemistry, University of Minnesota, Minneapolis, Minnesota 55455-0431, United States; orcid.org/0000-0001-8255-3853; Email: hillmyer@umn.edu

Christopher J. Ellison – Department of Chemical Engineering & Materials Science, University of Minnesota, Minneapolis, Minnesota 55455-0132, United States; orcid.org/0000-0002-0393-2941; Email: cellison@umn.edu

Authors

Hee Joong Kim — Department of Chemical Engineering & Materials Science, University of Minnesota, Minneapolis, Minnesota 55455-0132, United States; ⊚ orcid.org/0000-0001-6297-1636

Xiayu Peng — Department of Chemical Engineering & Materials Science, University of Minnesota, Minneapolis, Minnesota 55455-0132, United States; ⊙ orcid.org/0000-0002-6216-7493

Youngsu Shin — Department of Chemical Engineering & Materials Science, University of Minnesota, Minneapolis, Minnesota 55455-0132, United States

Complete contact information is available at: https://pubs.acs.org/10.1021/acs.jpcb.0c09322

Author Contributions

H.J.K. designed the overall experiments and wrote the manuscript. X.P. prepared the polymer blends, performed DSC and POM experiments, and provided feedback on the manuscript. Y.S. conducted FT-IR measurements. M.A.H. and C.J.E. led the project, helped devise experiments, interpreted data, and contributed to the manuscript.

Notes

The authors declare no competing financial interest.

■ ACKNOWLEDGMENTS

We acknowledge our principal funding source, the National Science Foundation Center for Sustainable Polymers at the University of Minnesota, which is a National Science Foundation supported Center for Chemical Innovation (CHE-1901635). We thank Yangming Kou for experimental support (XRD), and C. Maggie Lau, Charles J. McCutcheon, and Keiichiro Nomura for helpful feedback. We also thank Dr. David Giles for help with polymer film processing and his insight regarding hot press to make bubble-free samples.

■ REFERENCES

- (1) Cruz, C. A.; Barlow, J. W.; Paul, D. R. The basis for miscibility in polyester-polycarbonate blends. *Macromolecules* **1979**, *12*, 726–731.
- (2) Encyclopedia of Polymer Science and Engineering. 2nd ed.; Paul, D. R.; Barlow, J.; Keskkula, H., Eds.; Wiley & Sons: New York, 1988; Vol. 12; pp 399–461.
- (3) Suarez, H.; Barlow, J. W.; Paul, D. R. Mechanical-Properties of Abs Polycarbonate Blends. J. Appl. Polym. Sci. 1984, 29, 3253-3259.
- (4) Gaikwad, A. N.; Wood, E. R.; Ngai, T.; Lodge, T. P. Two calorimetric glass transitions in miscible blends containing poly-(ethylene oxide). *Macromolecules* **2008**, *41*, 2502–2508.
- (5) Lu, X.; Weiss, R. A. Relationship between the Glass-Transition Temperature and the Interaction Parameter of Miscible Binary Polymer Blends. *Macromolecules* **1992**, *25*, 3242–3246.
- (6) Manias, E.; Utracki, L. A. Thermodynamics of polymer blends. *Polym. Blends Handb.* **2014**, 171–289.

- (7) Hiemenz, P. C.; Lodge, T. P. Polymer chemistry; CRC Press: Florida, USA, 2007.
- (8) Kuo, S. W.; Chang, F. C. Miscibility and hydrogen bonding in blends of poly(vinylphenol-co-methyl methacrylate) with poly-(ethylene oxide). *Macromolecules* **2001**, *34*, 4089–4097.
- (9) Kadla, J. F.; Kubo, S. Miscibility and hydrogen bonding in blends of poly(ethylene oxide) and kraft lignin. *Macromolecules* **2003**, *36*, 7803–7811.
- (10) Kuo, S.-W. Hydrogen-bonding in polymer blends. *J. Polym. Res.* **2008**, *15*, 459–486.
- (11) Woo, E. M.; Barlow, J. W.; Paul, D. R. Miscible Blends of a Vinylidene-Chloride Vinyl-Chloride Co-Polymer with Aliphatic Polyesters. *J. Appl. Polym. Sci.* **1983**, 28, 1347–1360.
- (12) Smith, P.; Eisenberg, A. Ionomeric Blends. 1. Compatibilization of the Polystyrene Poly(Ethyl Acrylate) System Via Ionic Interactions. *J. Polym. Sci., Polym. Lett. Ed.* **1983**, 21, 223–230.
- (13) Polymer blends handbook; Utracki, L. A., Wilkie, C. A., Eds.; Springer: Dordrecht, 2002.
- (14) Idrees, M.; Jeelani, S.; Rangari, V. Three-Dimensional-Printed Sustainable Biochar-Recycled PET Composites. *ACS Sustainable Chem. Eng.* **2018**, *6*, 13940–13948.
- (15) Nomura, K.; Peng, X.; Kim, H.; Jin, K.; Kim, H. J.; Bratton, A. F.; Bond, C. R.; Broman, A. E.; Miller, K. M.; Ellison, C. J. Multiblock Copolymers for Recycling Polyethylene-Poly(ethylene terephthalate) Mixed Waste. ACS Appl. Mater. Interfaces 2020, 12, 9726–9735.
- (16) Avramova, N. Amorphous Poly(Ethylene-Terephthalate) Poly(Butylene Terephthalate) Blends Miscibility and Properties. *Polymer* **1995**, *36*, 801–808.
- (17) Escala, A.; Stein, R. S. Crystallization Studies of Blends of Polyethylene Terephthalate and Polybutylene Terephthalate. *Adv. Chem.* **1979**, *176*, 455–487.
- (18) Nassar, T. R.; Paul, D. R.; Barlow, J. W. Polyester-Polycarbonate Blends. 2. Poly(Ethylene-Terephthalate). *J. Appl. Polym. Sci.* **1979**, 23, 85–99.
- (19) Jo, W. H.; Lee, M. R.; Min, B. G.; Lee, M. S. Miscibility of Poly(Ether Imide) Poly(Ethylene-Terephthalate) Blends. *Polym. Bull.* **1994**, 33, 113–118.
- (20) Martinez, J. M.; Eguiazabal, J. I.; Nazabal, J. Miscibility level and properties of poly(ether imide)/poly(ethylene terephthalate) blends. *J. Appl. Polym. Sci.* **1996**, *62*, 393–408.
- (21) Rosenboom, J.-G.; Hohl, D. K.; Fleckenstein, P.; Storti, G.; Morbidelli, M. Bottle-grade polyethylene furanoate from ring-opening polymerisation of cyclic oligomers. *Nat. Commun.* **2018**, *9*, 2701.
- (22) Mialon, L.; Pemba, A. G.; Miller, S. A. Biorenewable polyethylene terephthalate mimics derived from lignin and acetic acid. *Green Chem.* **2010**, *12*, 1704–1706.
- (23) MacDonald, J. P.; Shaver, M. P. An aromatic/aliphatic polyester prepared via ring-opening polymerisation and its remarkably selective and cyclable depolymerisation to monomer. *Polym. Chem.* **2016**, *7*, 553–559.
- (24) Kim, H. J.; Reddi, Y.; Cramer, C. J.; Hillmyer, M. A.; Ellison, C. J. Readily Degradable Aromatic Polyesters from Salicylic Acid. *ACS Macro Lett.* **2020**, *9*, 96–102.
- (25) Baker, G. L.; Jing, R.; Smith, R. Degradable-1,4-benzodioxepin-3-hexyl-2,5-dione monomer derived polymer with a high glass transition temperature. U.S. Patent 7,923,528 B2, 2011.
- (26) Pedna, A.; Rosi, L.; Frediani, M.; Frediani, P. High glass transition temperature polyester coatings for the protection of stones. *J. Appl. Polym. Sci.* **2015**, *132*, 42323.
- (27) Saywell, C.; Mai, S.; Romeu, C.; Neves, J. C. L. Process for the production of poly(ethylene 2.5-furandicarboxylate) from 2.5-furandicarboxylic acid and use thereof, polyester compound and blends thereof. U.S. Patent 0,141,584 A1, 2015.
- (28) Poulopoulou, N.; Smyrnioti, D.; Nikolaidis, G. N.; Tsitsimaka, I.; Christodoulou, E.; Bikiaris, D. N.; Charitopoulou, M. A.; Achilias, D. S.; Kapnisti, M.; Papageorgiou, G. Z. Sustainable Plastics from Biomass: Blends of Polyesters Based on 2,5-Furandicarboxylic Acid. *Polymers* 2020, 12, 225.

- (29) Dupaix, R. B.; Boyce, M. C. Finite strain behavior of poly(ethylene terephthalate) (PET) and poly(ethylene terephthalate)-glycol (PETG). *Polymer* **2005**, *46*, 4827–4838.
- (30) Kuo, S.-W.; Huang, W.-J.; Huang, C.-F.; Chan, S.-C.; Chang, F.-C. Miscibility, specific interactions, and spherulite growth rates of binary poly(acetoxystyrene)/poly(ethylene oxide) blends. *Macromolecules* **2004**, *37*, 4164–4173.
- (31) Dargent, E.; Cabot, C.; Saiter, J. M.; Bayard, J.; Grenet, J. The glass transition Correlation of DSC and TSDC investigations. *J. Therm. Anal.* **1996**, *47*, 887–896.
- (32) Savin, D. A.; Larson, A. M.; Lodge, T. P. Effect of composition on the width of the calorimetric glass transition in polymer-solvent and solvent-solvent mixtures. *J. Polym. Sci., Part B: Polym. Phys.* **2004**, 42, 1155–1163.
- (33) Höhne, G. W. H.; Cammenga, H. K.; Eysel, W.; Gmelin, E.; Hemminger, W. The Temperature Calibration of Scanning Calorimeters. *Thermochim. Acta* **1990**, *160*, 1–12.
- (34) Wunderlich, B. Thermal Analysis of Polymeric Materials; Springer: Berlin, Heidelberg, New York, 2005.
- (35) Bell, J. P.; Dumbleton, J. H. Relation between Melting Behavior and Physical Structure in Polymers. *J. Polym. Sci., Part A-2* **1969**, *7*, 1033–1057.
- (36) Holdsworth, P. J.; Turner-Jones, A. Melting Behaviour of Heat Crystallized Poly(Ethylene Terephthalate). *Polymer* **1971**, *12*, 195–208
- (37) Fakirov, S.; Fischer, E. W.; Hoffmann, R.; Schmidt, G. F. Structure and Properties of Poly(Ethylene-Terephthalate) Crystallized by Annealing in Highly Oriented State. 2. Melting Behavior and Mosaic Block Structure of Crystalline Layers. *Polymer* 1977, 18, 1121–1129
- (38) Tan, S.; Su, A.; Li, W.; Zhou, E. New insight into melting and crystallization behavior in semicrystalline poly(ethylene terephthalate). *J. Polym. Sci., Part B: Polym. Phys.* **2000**, *38*, 53–60.
- (39) Marand, H.; Xu, J.; Srinivas, S. Determination of the equilibrium melting temperature of polymer crystals: Linear and nonlinear Hoffman-Weeks extrapolations. *Macromolecules* **1998**, *31*, 8219–8229.
- (40) Mark, J. E. Physical Properties of Polymers Handbook; Springer: Dordrecht, 2007.
- (41) Ziska, J. J.; Barlow, J. W.; Paul, D. R. Miscibility in PVC-Polyester Blends. *Polymer* 1981, 22, 918–923.
- (42) Moskala, E. J.; Howe, S. E.; Painter, P. C.; Coleman, M. M. On the Role of Intermolecular Hydrogen-Bonding in Miscible Polymer Blends. *Macromolecules* **1984**, *17*, 1671–1678.
- (43) Aubin, M.; Prud'homme, R. E. Analysis of the Glass-Transition Temperature of Miscible Polymer Blends. *Macromolecules* **1988**, *21*, 2945–2949.
- (44) Kalogeras, I. M. Encyclopedia of Polymer Blends; Isayev, A. I., Ed.; VCH: New York, 2016; vol.3; pp 1–134.
- (45) Kwei, T. K. The Effect of Hydrogen-Bonding on the Glass-Transition Temperatures of Polymer Mixtures. *J. Polym. Sci., Polym. Lett. Ed.* 1984, 22, 307–313.
- (46) Lin, A. A.; Kwei, T. K.; Reiser, A. On the Physical Meaning of the Kwei Equation for the Glass-Transition Temperature of Polymer Blends. *Macromolecules* **1989**, 22, 4112–4119.
- (47) Woo, E. M.; Mandal, T. K.; Chang, L. L.; Lee, S. C. Characterization of miscible poly(ethylene oxide) poly(phenyl methacrylate) system and the analysis of asymmetric T_g -composition dependence. *Polymer* **2000**, *41*, 6663–6670.
- (48) Kuo, S.-W.; Lin, C.-L.; Wu, H.-D.; Chang, F.-C. Thermal property and hydrogen bonding in blends of poly(vinylphenol) and poly(hydroxylether of bisphenol A). *J. Polym. Res.* **2003**, *10*, 87–93.
- (49) Iriarte, M.; Alberdi, M.; Shenoy, S. L.; Iruin, J. J. Excess specific heats in miscible binary blends with specific interactions. *Macromolecules* **1999**, *32*, *2661*–*2668*.
- (50) Huang, C.-F.; Chang, F.-C. Comparison of hydrogen bonding interaction between PMMA/PMAA blends and PMMA-co-PMAA copolymers. *Polymer* **2003**, *44*, 2965–2974.

- (51) Kuo, S. W.; Chang, F. C. Miscibility behavior and specific interaction of phenolic resin with poly(acetoxystyrene) blends. *Macromol. Chem. Phys.* **2002**, 203, 868–878.
- (52) Kuo, S. W.; Huang, C. F.; Chang, F. C. Study of hydrogen-bonding strength in poly(ε -caprolactone) blends by DSC and FTIR. *J. Polym. Sci., Part B: Polym. Phys.* **2001**, *39*, 1348–1359.
- (53) Roe, R.-J.; Zin, W.-C. Determination of the Polymer-Polymer Interaction Parameter for the Polystyrene-Polybutadiene Pair. *Macromolecules* **1980**, *13*, 1221–1228.
- (54) Meaurio, E.; Zuza, E.; Sarasua, J.-R. Miscibility and specific interactions in blends of poly(L-lactide) with poly(vinylphenol). *Macromolecules* **2005**, *38*, 1207–1215.
- (55) Nishi, T.; Wang, T. T. Melting point depression and kinetic effects of cooling on crystallization in poly (vinylidene fluoride)-poly (methyl methacrylate) mixtures. *Macromolecules* **1975**, *8*, 909–915.
- (56) Bell, J. P.; Murayama, T. Relations between Dynamic Mechanical Properties and Melting Behavior of Nylon-6,6 and Poly(Ethylene Terephthalate). *J. Polym. Sci., Part A-2* **1969**, 7, 1059–1073.
- (57) Groeninckx, G.; Reynaers, H.; Berghmans, H.; Smets, G. Morphology and melting behavior of semicrystalline poly(ethylene terephthalate). I. Isothermally crystallized PET. *J. Polym. Sci. Polym. Phys. Ed.* 1980, 18, 1311–1324.
- (58) Flory, P. J. Principles of Polymer Chemistry; Cornell University Press: New York, USA, 1953.
- (59) Imken, R. L.; Paul, D. R.; Barlow, J. W. Transition Behavior of Poly(Vinylidene Fluoride) Poly(Ethyl Methacrylate) Blends. *Polym. Eng. Sci.* **1976**, *16*, 593–601.
- (60) Gaur, U.; Lau, S. F.; Wunderlich, B. B.; Wunderlich, B. Heat-Capacity and Other Thermodynamic Properties of Linear Macromolecules. 8. Polyesters and Polyamides. *J. Phys. Chem. Ref. Data* 1983, 12, 65–89.
- (61) Huo, P. P.; Cebe, P. Melting-Point Depression in Poly-(Butylene Terephthalate)/Polyarylate Blends. *Macromolecules* **1993**, 26, 3127–3130.
- (62) Fredrickson, G. H.; Liu, A. J.; Bates, F. S. Entropic Corrections to the Flory-Huggins Theory of Polymer Blends Architectural and Conformational Effects. *Macromolecules* **1994**, *27*, 2503–2511.
- (63) Soria, V.; Figueruelo, J. E.; Campos, A. Polymer-Polymer Interaction Parameters in Solvent-Polymer-Polymer Ternary-Systems. *Eur. Polym. J.* **1981**, *17*, 137–143.
- (64) Vesely, D. Microstructural characterization of polymer blends. *Polym. Eng. Sci.* **1996**, *36*, 1586–1593.
- (65) Kuo, S.-W.; Chan, S.-C.; Chang, F.-C. Effect of hydrogen bonding strength on the microstructure and crystallization behavior of crystalline polymer blends. *Macromolecules* **2003**, *36*, 6653–6661.
- (66) Crist, B.; Schultz, J. M. Polymer spherulites: A critical review. *Prog. Polym. Sci.* **2016**, *56*, 1–63.
- (67) Yang, D. Z.; Hu, P. Miscibility, crystallization, and mechanical properties of poly(3-hydroxybutyrate) and poly(propylene carbonate) biodegradable blends. *J. Appl. Polym. Sci.* **2008**, *109*, 1635–1642.
- (68) Wang, Z.; Jiang, B. Crystallization kinetics in mixtures of poly(ε -caprolactone) and poly(styrene-co-acrylonitrile). *Macromolecules* **1997**, 30, 6223–6229.
- (69) Zhan, J.; Chen, Y.; Tang, G.; Pan, H.; Zhang, Q.; Song, L.; Hu, Y. Crystallization and Melting Properties of Poly(butylene succinate) Composites with Titanium Dioxide Nanotubes or Hydroxyapatite Nanorods. *J. Appl. Polym. Sci.* **2014**, *131*, 40335.
- (70) Eslamian, M.; Bagheri, R.; Pircheraghi, G. Co-crystallization in ternary polyethylene blends: tie crystal formation and mechanical properties improvement. *Polym. Int.* **2016**, *65*, 1405–1416.
- (71) Datta, J.; Nandi, A. K. Cocrystallization of poly(vinylidene fluoride) and vinylidene fluoride-tetrafluoro-ethylene copolymer blends. 3. Structural study. *Polymer* **1997**, 38, 2719–2724.
- (72) Hoffmann, S.; Vanhaecht, B.; Devroede, J.; Bras, W.; Koning, C. E.; Rastogi, S. Cocrystallization in piperazine-based polyamide copolymers: Small-and wide-angle X-ray diffraction studies at 30 °C. *Macromolecules* **2005**, *38*, 1797–1803.

- (73) Siegmann, A. Crystalline-Crystalline Polymer Blends Some Structure-Property Relationships. *J. Appl. Polym. Sci.* **1979**, 24, 2333—2345.
- (74) Varughese, K. T.; Nando, G. B.; De, S. K.; Sanyal, S. K. Tensile and Tear Failure of Plasticized Poly (Vinyl-Chloride) Epoxidized Natural-Rubber Miscible Blends. *J. Mater. Sci.* **1989**, 24, 3491–3496.
- (75) Bashford, D. Thermoplastics: Directory and Databook. Springer Science & Business Media, 1996.
- (76) Klimovica, K.; Pan, S.; Lin, T.-W.; Peng, X.; Ellison, C. J.; LaPointe, A. M.; Bates, F. S.; Coates, G. W. Compatibilization of iPP/HDPE Blends with PE-g-iPP Graft Copolymers. *ACS Macro Lett.* **2020**, *9*, 1161–1166.